

Evolutions of anisotropic universe on interacting holographic and new agegraphic scalar fields models of dark energy

Hossien Hossienkhani^{1,*} and Ali Aghamohammadi^{2,†}

¹*Hamedan Branch, Islamic Azad university, Hamedan, Iran*

²*Sanandaj Branch, Islamic Azad University, Sanandaj, Iran*

(Dated: December 3, 2024)

Abstract

Recently, the accelerated expansion of the universe is explained in cosmology models which many of them are based on the FRW framework. However, the early universe may not have been exactly uniform and the existence of anisotropy at early times is a natural phenomenon. In this work, a correspondence between the interacting new agegraphic dark energy models, the quintessence, tachyon and K-essence scalar fields on the anisotropic cosmological background are investigated. Given, the framework of the anisotropic model, both the dynamics and potential of these scalar field models according to the evolutionary behavior of the interacting new agegraphic dark energy models are reconstructed. Our numerical result show the effects of the interaction and anisotropic on the evolutionary behaviour the new agegraphic scalar field models.

keywords: Anisotropic universe-Holographic dark energy -New agegraphic- Scalar field

I. INTRODUCTION

Most remarkable observational discoveries in type-Ia supernovae (SN Iae) prevail that the universe has confirmed by two dark components containing dark energy (DE) and dark matter (DM) [1, 2]. DE, an unknown energy with large negative pressure, is utilized to explain the present cosmic accelerating expansion of the universe. The simplest candidate for DE is Einstein's cosmological constant (Λ) which is equivalent to the vacuum energy density in the universe and produces negative pressure with equation of state (EoS) parameter $\omega_\Lambda = -1$ since it fits the observational data well, but it suffers two well-known problems, i.e., "fine tuning problem" and "cosmic coincidence

*Electronic address: hossienhossienkhani@yahoo.com

†Electronic address: a.aqamohamadi@gmail.com, or, a.ghamohamadi@iausdj.ac.ir

problem”.

In order to understand the nature of DE phenomenon, various dynamical DE models have been investigated which can be delineated by the EoS parameter ω_Λ . It is well known that the holographic principle is an emergent result of the recent Studies for exploring the quantum gravity [3–5]. According to the holographic principle, the entropy of a system scales not with its volume, but with its surface area [6]. The holographic DE (HDE) was first proposed in [7] following the line of [8] where the infrared cut-off is taken to be the size of event horizon for DE. Ref. [8] purposed that the DE should obey this principle, thus its energy density has an upper limit and the fin-tuning problem for the cosmological constant is omitted. Its framework is the black hole thermodynamics [9] and the correspondence of the UV cut-of of a quantum field theory, which gives rise to the vacuum energy, with the distance of the theory [10, 11]. Li [7] and Hsu [12] formulated the acquired vacuum energy as HDE i.e. $\rho_\Lambda = 3c^2L^{-2}$, where c is a numerical constant and L is the infrared cutoff. If in a cosmological context we saturate this inequality by doing $L = H^{-1}$ [13], where H is the Hubble parameter, we obtain a model of holographic nature for the density of DE. Ref. [14] was presented a generalized and restored HDE in the braneworld context. The holographic phantom energy density grows rapidly and dominates the late time expanding phase, helping realize a cyclic universe scenario in Ref. [15].

Another plan to explore the nature of DE, dubbed agegraphic DE (ADE), has been proposed [16] which explain the acceleration of the universe expansion with the gravitational effect in general relativity. In the ADE models the age of the universe is taken the length measure instead of the horizon distance, so the causality problem that appears in the HDE model can be avoided [17]. After introducing the ADE model by Cai [16], a new model of agegraphic DE (NADE) was proposed in Ref. [18], while the time scale is chosen to be the conformal time η instead of the age of the universe i.e. T . The ADE undergo from the difficulty to characterize the matter dominated era [18] while the NADE resolved this subject [19]. Many authors did some detailed study of this NADE model [20–24].

A Bianchi type I (BI) universe, being the straightforward generalization of the flat FLRW universe, is of interest because it is one of the simplest models of a non-isotropic universe exhibiting a homogeneity and spatial flatness. In this case, unlike the FLRW universe which has the same scale factor for three spatial directions, a BI universe has a different scale factor for each direction. This fact introduce a non-isotropy to the system. The possible effects of anisotropy in the early universe have been investigated with BI models from different points of view [25–28]. Therefore, we establish a correspondence between the interacting holographic and new agegraphic DE scalar

field in an anisotropic universe.

The organisation of this work is as follows. In the next section, a brief review of the general formulation of the field equations in a BI metric are discussed, then, interacting DE with cold DM (CDM) in a non-isotropic BI universe is studied. The Sec. III is concerned with interacting HDE with the quintessence, tachyon and K-essence scalar field in an anisotropic universe. The Sec. IV, is related to establish the correspondence between the model of interacting NADE and the quintessence, tachyon and K-essence DE in BI model. At last the Sec. V is devoted to conclusion and discussion.

II. GENERAL FRAMEWORK

Bianchi cosmologies are spatially homogeneous but not necessarily isotropic. Here we will consider BI cosmology. The metric of this model is given by

$$ds^2 = dt^2 - A^2(t)dx^2 - B^2(t)dy^2 - C^2(t)dz^2, \quad (1)$$

where the metric functions, A, B, C , are merely functions of time, t . However, the underlying Lie algebra of the isometry group of the BI metrics is completely different [29]. The contribution of the interaction with the matter fields is given by the energy momentum tensor which is defined as

$$T_{\nu}^{\mu} = \text{diag}[\rho, -\omega\rho, -\omega\rho, -\omega\rho], \quad (2)$$

where ρ and ω represent the energy density and EoS parameter, respectively. The field equations for the axially symmetric BI metric are [30–32]:

$$3H^2 - \sigma^2 = \frac{1}{M_p^2}(\rho_m + \rho_\Lambda), \quad (3)$$

$$3H^2 + 2\dot{H} + \sigma^2 = -\frac{1}{M_p^2}(p_m + p_\Lambda), \quad (4)$$

$$\dot{\sigma} + \theta\sigma = 0, \quad (5)$$

where $M_p^2 = 1/(8\pi G)$, ρ_Λ and p_Λ are the Planck mass, the energy density and pressure of DE, respectively, and $a = (ABC)^{\frac{1}{3}}$ is the scale factor, and $\sigma^2 = 1/2\sigma_{ij}\sigma^{ij}$ in which $\sigma_{ij} = u_{i,j} + \frac{1}{2}(u_{i;k}u^k u_j + u_{j;k}u^k u_i) + \frac{1}{3}\theta(g_{ij} + u_i u_j)$ is the shear tensor ($\sigma_{ij}u^j = 0, \sigma^i_i = 0$), which describes the rate of distortion of the matter flow, and $\theta = 3H = u^j_{,j}$ is the scalar expansion, where u^j is 4-velocity. In a co-moving coordinate system, i.e. ($u^i = \delta_0^i$). From (5) it is easy to give a non-correct interpretation for the shear dynamics because we could conclude shear tensor is equal to a

constant times a^{-3} . Using Eq. (3), the dimensionless density parameter of BI can also be defined as usual

$$\Omega_m = \frac{\rho_{m0}}{\rho_{cr}}, \quad \Omega_\Lambda = \frac{\rho_\Lambda}{\rho_{cr}}, \quad \Omega_\sigma = \frac{\sigma^2}{3H^2}, \quad (6)$$

where the critical energy density is $\rho_{cr} = 3M_p^2 H^2$. Using Eq. (6), we can rewrite (3) in the form of fractional energy densities as

$$\Omega_m + \Omega_\Lambda = 1 - \Omega_\sigma. \quad (7)$$

The above equation shows that the sum of the energy density parameters approaches 1 at late times. So at late times the universe becomes flat. Therefore for sufficiently large time, this model predicts that the anisotropy of the universe will damp out and universe will become isotropic. This result also shows that in the early universe i.e. during the radiation and matter dominated era the universe was anisotropic and the universe approaches to isotropy as DE starts to dominate the energy density of the universe. When isotropic is assumed, $\Omega_m + \Omega_\Lambda = 1$, and the model has only one free parameter, Ω_Λ . We assume that the DE is coupled with DM, in such way that total energy-momentum is still conserved. In the flat BI cosmology with a scale factor a , the continuity equations for both components are [33]

$$\dot{\rho}_\Lambda + 3H\rho_\Lambda(1 + \omega_\Lambda) = -Q, \quad (8)$$

$$\dot{\rho}_m + 3H\rho_m = Q, \quad (9)$$

where $\omega_\Lambda = p_\Lambda/\rho_\Lambda$ is the EoS parameter of the interacting DE and Q is the interaction term. The case $Q > 0$ ($Q < 0$) corresponds to either DE transformation into DM and vice versa of the model. Following [10, 11], we shall assume $Q = 3b^2 H(\rho_m + \rho_\Lambda)$ with the coupling constant b^2 .

In the following, we will find a form for the function $V(\phi)$ which is able to reconstruct HDE and NADE models as following.

III. HDE WITH HUBBLE RADIUS AS IR CUTOFF IN BI MODEL

First we will consider the size L as the Hubble radius H^{-1} , thus the energy density for the DE becomes [3, 34, 35]

$$\rho_\Lambda = 3c^2 M_p^2 H^2, \quad (10)$$

where c^2 is a constant. As it is well known, different possibilities have been tried to varying degrees of success, namely, the particle horizon [36], the future event horizon [7, 10] and the Hubble horizon

[13]. Hence, in this work, we set the Hubble radius as the infrared cutoff $L = H^{-1}$ [37]. Taking the time derivative of relation (10) and using the BI equation we find

$$\dot{\rho}_\Lambda = 2\rho_\Lambda \frac{\dot{H}}{H} = -3Hc^2 [2M_p^2\sigma^2 + \rho_\Lambda(1 + \omega_\Lambda + r)], \quad (11)$$

where $r = \rho_m/\rho_\Lambda = (1 - \Omega_\sigma - \Omega_\Lambda)/\Omega_\Lambda$ is the energy density ratio. Substituting Eq. (11) into (8), the EoS parameter for interaction HDE is given by

$$\omega_\Lambda = \frac{\Omega_\sigma}{1 - c^2} - \frac{b^2(1 - \Omega_\sigma)}{c^2(1 - c^2)}. \quad (12)$$

This relation shows that the EoS parameter is depend on b^2 , c and Ω_σ parameter. Therefore, ω_Λ becomes a constant. In the absence of interaction between HDE and CDM, $b^2 = 0$ we have $\omega_\Lambda = \Omega_\sigma/(1 - c^2)$. It may be pointed out here that if one sets $\Omega_\sigma = 0$ Eq. (12) reduce to that obtained for a flat FRW universe.

Now, we intend to categorize our study into three types of the model, i.e. quintessence, tachyon and K-essence models in non-isotropic universe.

A. Quintessence reconstruction of HDE in BI

The ordinary scalar field ϕ is governed by quintessence which is minimally coupled with gravity. We treat HDE as an ordinary quintessence scalar field ϕ . Thus, we have

$$\rho_\phi = \frac{1}{2}\dot{\phi}^2 + V(\phi), \quad (13)$$

$$p_\phi = \frac{1}{2}\dot{\phi}^2 - V(\phi), \quad (14)$$

where $\dot{\phi}^2$ and $V(\phi)$ are termed as kinetic energy and scalar potential, respectively. Furthermore, we obtain

$$V(\phi) = \frac{1 - \omega_\phi}{2}\rho_\phi, \quad (15)$$

$$\dot{\phi}^2 = (1 + \omega_\phi)\rho_\phi, \quad (16)$$

where $\omega_\phi = p_\phi/\rho_\phi$. For the accelerated expansion of the universe, the EoS parameter for quintessence must be less than $-1/3$. By means of $\rho_\phi = \rho_\Lambda$ and $\omega_\phi = \omega_\Lambda$ and substituting Eqs. (10) and (12) into (16) one can get

$$\phi = cM_p \left[3 \left(1 + \frac{\Omega_\sigma}{1 - c^2} - \frac{b^2(1 - \Omega_\sigma)}{c^2(1 - c^2)} \right) \right]^{\frac{1}{2}} \ln a. \quad (17)$$

By using Eqs. (3), (6), (10) and (12) we obtain

$$\frac{\dot{H}}{H^2} = -\frac{3}{2} \left(1 - \frac{b^2(1-\Omega_\sigma)}{c^2(1-c^2)} + \frac{1+\Omega_\sigma}{1-c^2} \right). \quad (18)$$

Integration of Eq. (18), the scaler field (17) can be written

$$\phi = \frac{2cM_p}{\sqrt{3}} \frac{\left(1 + \frac{\Omega_\sigma}{1-c^2} - \frac{b^2(1-\Omega_\sigma)}{c^2(1-c^2)} \right)^{\frac{1}{2}}}{1 - \frac{b^2(1-\Omega_\sigma)}{c^2(1-c^2)} + \frac{1+\Omega_\sigma}{1-c^2}} \ln t, \quad (19)$$

and the potential

$$V(\phi) = \frac{2c^2 M_p^2}{3} \left[\frac{1 - \frac{\Omega_\sigma}{1-c^2} + \frac{b^2(1-\Omega_\sigma)}{c^2(1-c^2)}}{\left(1 - \frac{b^2(1-\Omega_\sigma)}{c^2(1-c^2)} + \frac{1+\Omega_\sigma}{1-c^2} \right)^2} \right] \exp \left[-\frac{\sqrt{3}\phi}{cM_p} \frac{1 - \frac{b^2(1-\Omega_\sigma)}{c^2(1-c^2)} + \frac{1+\Omega_\sigma}{1-c^2}}{\left(1 + \frac{\Omega_\sigma}{1-c^2} - \frac{b^2(1-\Omega_\sigma)}{c^2(1-c^2)} \right)^{\frac{1}{2}}} \right]. \quad (20)$$

From the solution of (18), it is readily given the scale factor is $a = t^{\frac{2}{3}} \left(1 - \frac{b^2(1-\Omega_\sigma)}{c^2(1-c^2)} + \frac{1+\Omega_\sigma}{1-c^2} \right)^{-1}$. It clear that an accelerated universe $b^2 > c^2/3(4 + 3\Omega_\sigma - c^2)$ can be obtained when $\ddot{a} > 0$.

B. Tachyon reconstruction of HDE in BI

The tachyon model, originated from the string theory, has been suggested to explain DE scenario. It has an interesting feature that a rolling tachyon interpolates the EoS parameter between -1 to 0 . Also, the tachyon model is the best candidate for inflation at high energy. In a flat BI background the energy density and the pressure density are given by [38–40]

$$\rho_T = -T_0^0 = \frac{V(\phi)}{\sqrt{1-\dot{\phi}^2}}, \quad (21)$$

$$p_T = T_i^i = -V(\phi)\sqrt{1-\dot{\phi}^2}. \quad (22)$$

The EoS of the tachyon is given by

$$\omega_T = \dot{\phi}^2 - 1. \quad (23)$$

In the following, one can express ϕ in terms of b^2 , c^2 and Ω_σ . Hence, by equating (12) with (23), i.e. $\omega_\Lambda = \omega_T$, which gives

$$\phi(t) = \left(1 + \frac{\Omega_\sigma}{1-c^2} - \frac{b^2(1-\Omega_\sigma)}{c^2(1-c^2)} \right)^{\frac{1}{2}} t. \quad (24)$$

Then we find that $V(\phi)$ can be expressed in term of H

$$V(\phi) = 3c^2 M_p^2 H^2 \left(-\frac{\Omega_\sigma}{1-c^2} + \frac{b^2(1-\Omega_\sigma)}{c^2(1-c^2)} \right)^{\frac{1}{2}}. \quad (25)$$

Integrating of Eq. (18) and using (25) we obtain tachyon potential in term of the scalar field

$$V(\phi) = \frac{4c^2 M_p^2}{3\phi^2} \left(-\frac{\Omega_\sigma}{1-c^2} + \frac{b^2(1-\Omega_\sigma)}{c^2(1-c^2)} \right)^{\frac{1}{2}} \frac{1 + \frac{\Omega_\sigma}{1-c^2} - \frac{b^2(1-\Omega_\sigma)}{c^2(1-c^2)}}{\left(1 - \frac{b^2(1-\Omega_\sigma)}{c^2(1-c^2)} + \frac{1+\Omega_\sigma}{1-c^2} \right)^2}. \quad (26)$$

In this case the evolution of the tachyon is as $\phi \propto t$. Tachyon potentials, which are not steep compared to $V(\phi) \propto \phi^{-2}$ lead to an accelerated expansion [41].

C. K-essence reconstruction of HDE in BI

The K-essence model is different from quintessence scalar field model in the sense that it evolves the universe in the accelerated expansion era. It is originated from the idea of K-inflation which was used to describe the inflation of the early universe at high energies [42]. This kind of models is characterized by non-canonical kinetic energy terms, and are described by a general scalar field action which is a function of ϕ and $\chi = \dot{\phi}^2/2$, and is given by [43]

$$S = \int d^4x \sqrt{-g} P(\phi, \chi), \quad (27)$$

where $P(\phi, \chi)$ is an arbitrary function of ϕ and its kinetic energy χ . Based on the analysis of the Lagrangian density, it can be transformed into

$$P(\phi, \chi) = f(\phi)(-\chi + \chi^2), \quad (28)$$

and the energy density in these models is given by

$$\rho(\phi, \chi) = f(\phi)(-\chi + 3\chi^2). \quad (29)$$

And the EoS parameter $\omega_K = P(\phi, \chi)/\rho(\phi, \chi)$ is

$$\omega_K = \frac{\chi - 1}{3\chi - 1}. \quad (30)$$

This shows that ω_K does not change for the fix χ . Equating $\omega_K = \omega_\Lambda$ from Eq. (12) and (30), we get

$$\chi = \frac{b^2(1-\Omega_\sigma) + c^2(1-c^2-\Omega_\sigma)}{3b^2(1-\Omega_\sigma) + c^2(1-c^2-3\Omega_\sigma)}. \quad (31)$$

The EoS parameter in Eq. (30) diverges for $\chi = 1/3$. For the case of $\chi > 1/3$, the condition $\omega_K < -1/3$ leads to a high bound on $\chi < 2/3$. The requirement of an accelerated expansion gives $1/3 < \chi < 2/3$ and the cosmological constant limit corresponds to $\chi = 1/2$. As we have demanded

that the EoS parameter be positive, Eq. (30) implies that $\chi - 1 < -2/3 < 0$. Using Eq. (31) and $\chi = \dot{\phi}^2/2$, we obtain

$$\dot{\phi}^2 = 2 \frac{b^2(1 - \Omega_\sigma) + c^2(1 - c^2 - \Omega_\sigma)}{3b^2(1 - \Omega_\sigma) + c^2(1 - c^2 - 3\Omega_\sigma)}, \quad (32)$$

Turning to the cosmic time variable one can write the equation for the K-essence field as follows

$$\phi(t) = \left(2 \frac{b^2(1 - \Omega_\sigma) + c^2(1 - c^2 - \Omega_\sigma)}{3b^2(1 - \Omega_\sigma) + c^2(1 - c^2 - 3\Omega_\sigma)} \right)^{\frac{1}{2}} t. \quad (33)$$

Note that the field increases with the increment of t . From Eqs. (29) and (31) it can be obtained an expression for the k-essence potential $f(\phi)$ in terms of the ϕ

$$f(\phi) = \frac{4M_p^2}{9\phi^2} \frac{3b^2(1 - \Omega_\sigma) + c^2(1 - c^2 - 3\Omega_\sigma)}{1 - c^2} \left(1 - \frac{b^2(1 - \Omega_\sigma)}{c^2(1 - c^2)} + \frac{1 + \Omega_\sigma}{1 - c^2} \right)^{-2}, \quad (34)$$

where the Eq. (30) was used. From Eq. (32) we see that the kinetic energy of K-essence becomes constant, but it can take different values based on magnitude of b , c and Ω_σ parameter, although ϕ is not constant and is variable with cosmic time.

IV. NADE WITH SCALAR FIELD IN BI MODEL

The energy density of the NADE can be written

$$\rho_\Lambda = \frac{3n^2 M_p^2}{\eta^2}, \quad (35)$$

where the numerical factor $3n^2$ has been introduced to parameterize some uncertainties, such as the species of quantum fields in the universe, or the effect of curved space-time. The conformal time is given by

$$\eta = \int \frac{dt}{a(t)} = \int \frac{da}{Ha^2}. \quad (36)$$

If we write η to be a definite integral, there will be an integral constant in addition. Thus, we have $\dot{\eta} = 1/a$. The energy density parameter of the NADE is now given by

$$\Omega_\Lambda = \frac{n^2}{H^2 \eta^2}. \quad (37)$$

Taking the derivative of Eq. (35) with respect to the cosmic time and using (37) we get

$$\dot{\rho}_\Lambda = -2H \frac{\sqrt{\Omega_\Lambda}}{na} \rho_\Lambda. \quad (38)$$

Inserting this relation into (8) we obtain the EoS parameter of the interacting NADE

$$\omega_\Lambda = -1 + \frac{2}{3na} \sqrt{\Omega_\Lambda} - \frac{b^2}{\Omega_\Lambda} (1 - \Omega_\sigma). \quad (39)$$

It is important to note that when $b^2 = 0$, the interacting DE becomes trivial and Eq. (39) reduces to its respective expression in new ADE in general relativity [30]

$$\omega_\Lambda = -1 + \frac{2\sqrt{\Omega_\Lambda}}{3na}. \quad (40)$$

In this case ($b^2 = 0$), the present accelerated expansion of our universe can be derived only if

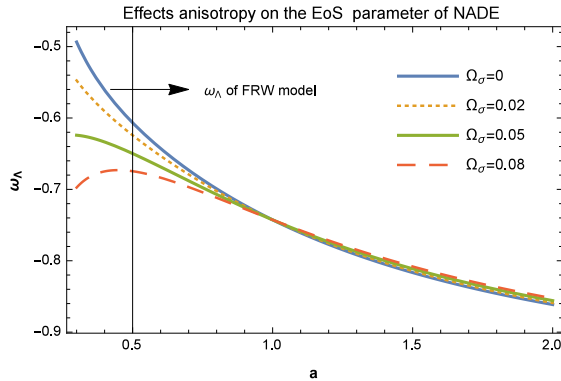


FIG. 1: The plot shows the evolution of the EoS parameter of NADE, Eq. (39), for different the anisotropy energy density parameter Ω_σ . Auxiliary parameters are $\Omega_{m0} = 0.274$ [25], $n = 2$ and $b^2 = 0.02$.

$n > 1$ [18], in addition, we see that the EoS parameter translates the universe from vacuum DE region towards quintessence region; eventually, for the case of matter dominated era $\omega_\Lambda = -2/3$ whilst $\Omega_\Lambda = n^2 a^2/4$ and in the radiation dominated era $\omega_\Lambda = -1/3$ whilst $\Omega_\Lambda = n^2 a^2$. We test this scenario for the interaction between NADE and DM by using some observational results. For the comparison with the phenomenological interacting model, in our scenario the coupling between NADE and DM can be expressed by b^2 parameter as in the phenomenological interaction form. In fact, b^2 is within the region of the golden supernova data fitting result $b^2 = 0.00^{+0.11}_{-0.00}$ [10] and the observed CMB low l data constraint [44]. We plot the EoS parameter ω_Λ versus a with respect to different choices of anisotropy energy density parameter Ω_σ , i.e., 0, 0.02, 0.05, 0.08 shown in Figure 1. It clear that the EoS parameter decrease with the scale factor increase and the effect of various Ω_σ are negligible but as $a \rightarrow 0$, it is clear that increasing of the Ω_σ cause to decrease the EoS parameter. Another best fit data with the NADE model is $n = 2.886^{+0.084}_{-0.082}$ at the 1σ level and $n = 2.886^{+0.169}_{-0.163}$ at the 2σ level [24], $n = 2.807^{+0.087}_{-0.086}(1\sigma)^{+0.176}_{-0.170}(2\sigma)$ [45], for a flat universe $n = 2.76^{+0.111}_{-0.109}$ [19] and for the non-flat universe $n = 2.673^{+0.053+0.127+0.199}_{-0.077-0.151-0.222}$ [46]. For the Λ CDM

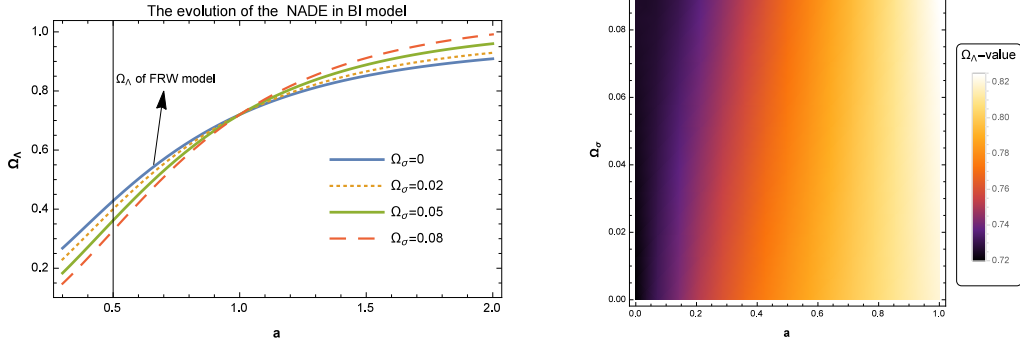


FIG. 2: The plot shows the evolution of the NADE density parameter, Eq. (44), for different value of the Ω_σ . Auxiliary parameters are $\Omega_{m0} = 0.274$ [25], $n = 2$ and $b^2 = 0.02$.

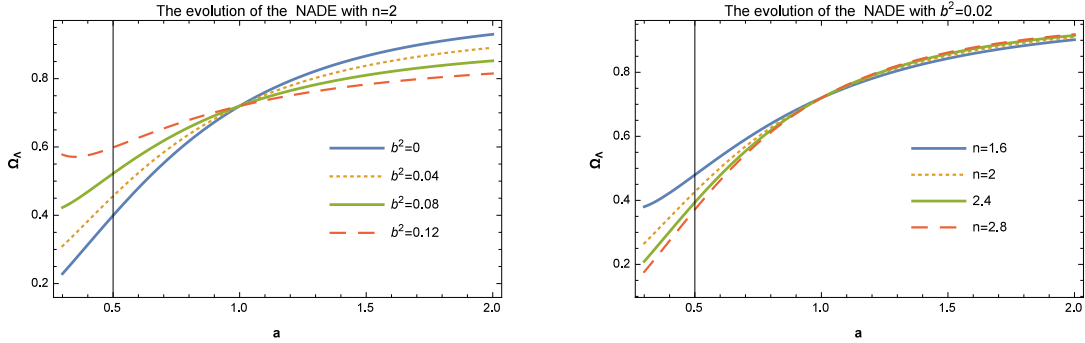


FIG. 3: Left figure representations of ω_Λ for the NADE with a for different value of the b^2 with $n = 2$ while right figure representations of ω_Λ versus a for various model parameters n and b^2 . For both cases, we take $\Omega_{m0} = 0.274$ [25] and $\Omega_\sigma = 0.001$.

cosmology, $\Omega_{m0} = 0.274$ is given by the WMAP five-year observations [25]. In what follows given to the Eq. (39) and its evaluations in the Fig. 1, by pick $b^2 \neq 0$, taking account $\Omega_{m0} = 0.274$ [25], $\Omega_{\Lambda 0} = 1 - (\Omega_{m0} + \Omega_\sigma)$, $\Omega_\sigma = 0.001$, $n = 2.7$ [19] and $a = 1$ for the present time, Eq. (39) gives

$$\omega_\Lambda = -0.789 - 1.37b^2, \quad (41)$$

where is clear that the phantom EoS $\omega_\Lambda < -1$ can be achieved by set $b^2 > 0.15$ for the coupling between NADE and CDM. In the future, where $a \rightarrow \infty$, $\omega_\Lambda < -1$ for $b^2 > 0$, i.e. it may be the ω_Λ crosses the phantom divide line in the presence interacting DM and DE. We can also obtain the evolution behavior of the dark energy. Taking the time derivative of Ω_Λ in Eq. (37) and relation $\dot{\Omega}_\Lambda = H\Omega'_\Lambda$, give

$$\Omega'_\Lambda = -2\Omega_\Lambda \left(\frac{\dot{H}}{H^2} + \frac{\sqrt{\Omega_\Lambda}}{na} \right). \quad (42)$$

Taking the derivative of the BI equation (3) with respect to the cosmic time, and using Eqs. (7), (8), (35) and (37), it is easy to find

$$\frac{\dot{H}}{H^2} = -\frac{3}{2}(1 - \Omega_\Lambda + \Omega_\sigma) - \frac{\Omega_\Lambda^{\frac{3}{2}}}{na} + \frac{3}{2}b^2(1 - \Omega_\sigma). \quad (43)$$

Combining Eqs. (42) and (43), we have the equation of motion, a differential equation, for Ω_Λ

$$\Omega'_\Lambda = 3\Omega_\Lambda \left(\Omega_\sigma + (1 - \Omega_\Lambda) \left(1 - \frac{2}{3na} \sqrt{\Omega_\Lambda} \right) - b^2(1 - \Omega_\sigma) \right). \quad (44)$$

As shown in Ref. [18], the parameters n and Ω_{m0} are not independent of each other. If one takes

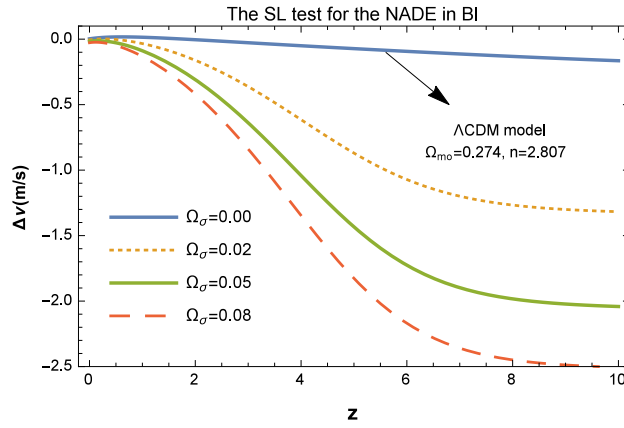


FIG. 4: The SL test for the NADE model for four different value of the anisotropy energy density parameter Ω_σ and the Λ CDM model with $\Omega_{m0} = 0.274$, $b^2 = 0.02$ and $n = 2.807$.

them as free parameters, the NADE model will become confused. Therefore the initial conditions in NADE should be taken at the early times. Alike Ref. [18] proposed the initial condition for the case of ADE, $\Omega_\Lambda = n^2 a^2 / 4$, at $z = 1/a - 1 = 2000$, so Eq. (44) can be numerically solved. The numerical results obtained for Ω_Λ are plotted in the Figs. 2 and 3 for different value of the Ω_σ , b^2 and n , respectively. Figure 2 show the effects of the anisotropic on the evolutionary behaviour the NADE model. Also, Figures illustrates the Ω_Λ increase with the a increase but: I) increase of the Ω_σ cause the Ω_Λ increases with sharper slope. II) Increasing the coefficient coupling cause the early and final Ω_Λ values to ($a \ll (>>)$) increases (decreases) respectively III) at last, increase of n parameter cause the Ω_Λ parameter pick smaller value for the smaller scale factor i.e. $a \ll$.

Ref. [47] introduced the redshift relation by the a spectroscopic velocity shift $\Delta\nu$ as $\Delta\nu \equiv \Delta z / (1 + z)$ where $z = 1/a - 1$. By using the Hubble parameter $H(z) = -\dot{z} / (1 + z)$ and Eq. (3), we obtain

$$\Delta\nu = H_0 \Delta t_0 \left(1 - (1 + z)^{-1} \left(\frac{\Omega_{m0}(1 + z)^3 + \Omega_{\sigma0}(1 + z)^6}{1 - \Omega_\Lambda} \right)^{\frac{1}{2}} \right), \quad (45)$$

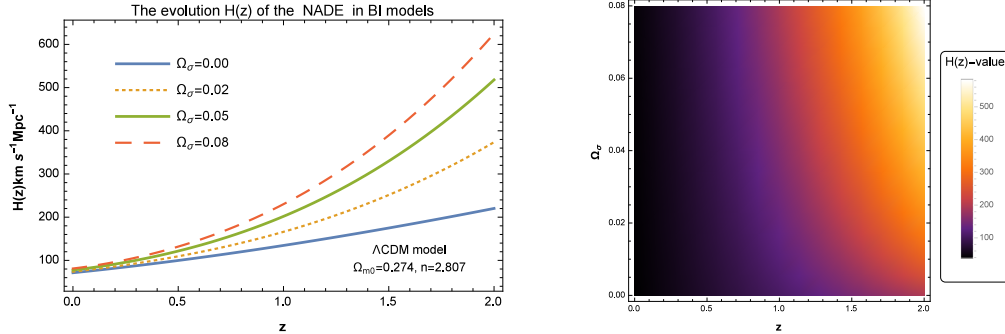


FIG. 5: The evolution of $H(z)$ versus redshift z in NADE anisotropic universe for different values of parameter Ω_σ with $n = 2.807$, $\Omega_{m0} = 0.274$ [25], $H_0 = 72 \text{ km s}^{-1} \text{ Mpc}^{-1}$ and $b^2 = 0.02$.

where we set $\Delta t_0 = 10$ years. We will examine the Sandage-Loeb (SL) test, and then examine effects of anisotropy on the NADE in the SL test. To do this we reconstruct the velocity shift behavior in the NADE model respect z for different value of the Ω_σ in Fig . 4. We have chosen the fractional matter density $\Omega_{m0} = 0.274$ from ΛCDM [25] and $n = 2.807$ [45]. From Fig. 4 we see that the NADE in BI model can be distinguished from the ΛCDM model via the SL test. Beside the amplitude and slope of the signal depend mainly on Ω_σ .

To constrain cosmological parameters we plot the $H(z)$ and effects of anisotropy on NADE for the cases of $n = 2.807$, $\Omega_{m0} = 0.274$ [25], $H_0 = 72 \text{ km s}^{-1} \text{ Mpc}^{-1}$ and $b^2 = 0.02$ that is shown in Figure 5. The value of $H(z)$ is then directly computed by using Eq. (3). From Fig. 5, we can clearly see that for different Ω_σ parameter value the process of cosmic evolution looks quite similar, i.e., for the bigger value the Ω_σ parameter is taken, the bigger value the Hubble expansion rate $H(z)$ is gotten. For this model, we consider, $H_0 = 72 \text{ km s}^{-1} \text{ Mpc}^{-1}$, as the value of $H_0 = 73 \pm 3 \text{ km s}^{-1} \text{ Mpc}^{-1}$ from the combination WMAP 3 year estimate [48], and the other with $H_0 = 68 \pm 4 \text{ km s}^{-1} \text{ Mpc}^{-1}$ from a median statistics analysis of 461 [49].

A. Quintessence reconstruction of NADE in BI

Now we suggest a correspondence between the new agegraphic dark energy and quintessence scalar field namely, we identify ρ_ϕ to be ρ_Λ . Using relation $\rho_\phi = \rho_\Lambda = 3M_p^2 H^2 \Omega_\Lambda$ and substituting Eqs. (37) and (39) into (15) and (16) one can readily find the kinetic energy term and the potential

term as

$$\dot{\phi}^2 = M_p^2 H^2 \left(\frac{2}{na} \Omega_\Lambda^{\frac{3}{2}} - 3b^2(1 - \Omega_\sigma) \right), \quad (46)$$

$$V(\phi) = M_p^2 H^2 \left(3\Omega_\Lambda + \frac{3b^2}{2}(1 - \Omega_\sigma) - \frac{\Omega_\Lambda^{\frac{3}{2}}}{na} \right). \quad (47)$$

From definition $\dot{\phi} = H\phi'$, one can rewrite Eq. (46) as

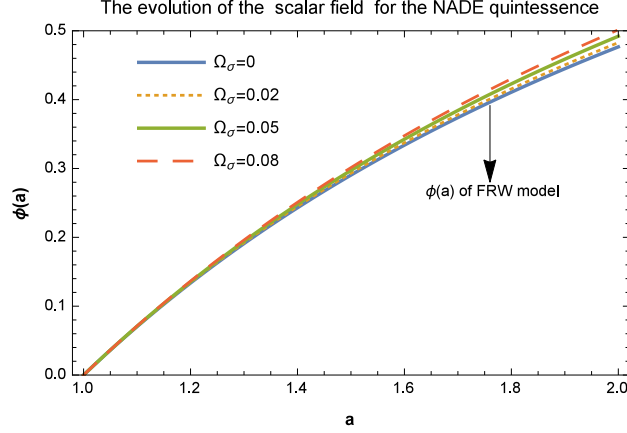


FIG. 6: The plot shows the evolution of the NADE quintessence scalar field, Eq. (48), for four different values of the anisotropy energy density parameter Ω_σ . Auxiliary parameters are $\Omega_\Lambda^0 = 0.72$, $b^2 = 0.02$, $n = 2$ and $\phi(1)=0$.

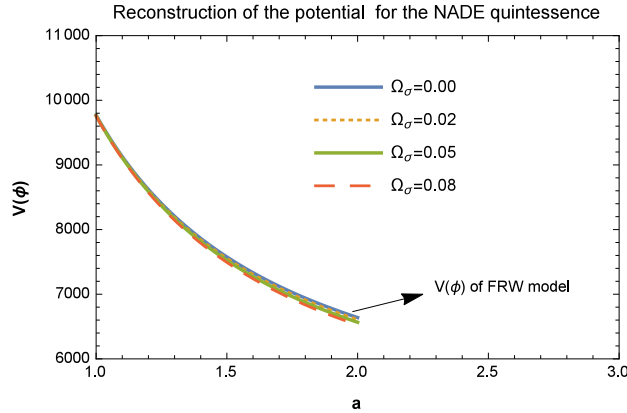


FIG. 7: The plot shows the NADE quintessence potential, Eq. (47), versus the scale factor for different Ω_σ . Auxiliary parameters as in Fig. 6.

$$\phi' = M_p \left(\frac{2}{na} \Omega_\Lambda^{\frac{3}{2}} - 3b^2(1 - \Omega_\sigma) \right)^{\frac{1}{2}}. \quad (48)$$

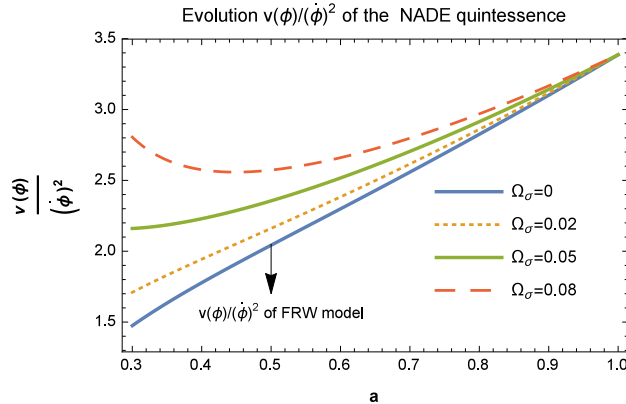


FIG. 8: The plot shows the NADE quintessence $\frac{V(\phi)}{\dot{\phi}^2}$, for four different value of Ω_σ . Auxiliary parameters as in Fig. 6.

Therefore, we have established an interacting new agegraphic quintessence dark energy model and reconstructed the potential of the agegraphic quintessence as well as the dynamics of scalar field in an anisotropic universe. Basically, from Eqs. (44) and (48) one can derive $\phi = \phi(a)$ and then combining the result with (47) one finds $V = V(\phi)$. Unfortunately, the analytical form of the potential in terms of the new agegraphic quintessence field cannot be determined due to the complexity of the equations involved. However, we can obtain it numerically. The evolution of the NADE quintessence scalar field, Eq. (48), for four different values of Ω_σ is plotted in Fig. 6. Figure 6 shows that the scalar field increases (and hence the kinetic energy $\dot{\phi}^2$ of the potential decreases) with the passage of time. The potential V versus a for four different value of the Ω_σ are shown in Figure 7, indicating the decreasing behavior. It illustrate for a given Ω_σ , V decreases with increasing a and the curve is shifted to the smaller values of V with increasing the Ω_σ . Also, we see from these figures that the cosmic evolution trends are quite similar for these four anisotropy energy density parameters. The evolution of $V(\phi)/\dot{\phi}^2$ versus Ω_Λ is illustrated in Fig. 8. It illustrate fraction of potential per kinetic energy increase with the Ω_Λ increase and its magnitude increase with the Ω_σ increase for the smaller Ω_Λ .

B. Tachyon reconstruction of NADE in BI

Next, we reconstruct the new agegraphic tachyon DE model, connecting the tachyon scalar field with the NADE in BI universe. Using Eqs. (37) and (39) one can easily show that the tachyon

potential and kinetic energy term take the following form

$$V(\phi) = 3M_p^2 H^2 \Omega_\Lambda \left(1 - \frac{2}{3na} \sqrt{\Omega_\Lambda} + \frac{b^2}{\Omega_\Lambda} (1 - \Omega_\sigma) \right)^{\frac{1}{2}}, \quad (49)$$

$$\dot{\phi} = \left(\frac{2}{3na} \sqrt{\Omega_\Lambda} - \frac{b^2}{\Omega_\Lambda} (1 - \Omega_\sigma) \right)^{\frac{1}{2}}. \quad (50)$$

Therefore the evolution behavior of the tachyon field can be obtained by integrating the above equation

$$\phi(a) - \phi(1) = \int_1^a \frac{1}{Ha} \sqrt{\frac{2}{3na} \sqrt{\Omega_\Lambda} - \frac{b^2}{\Omega_\Lambda} (1 - \Omega_\sigma)} da, \quad (51)$$

where Ω_Λ is given by Eq. (44). The evolutionary form of the tachyon field and the reconstructed

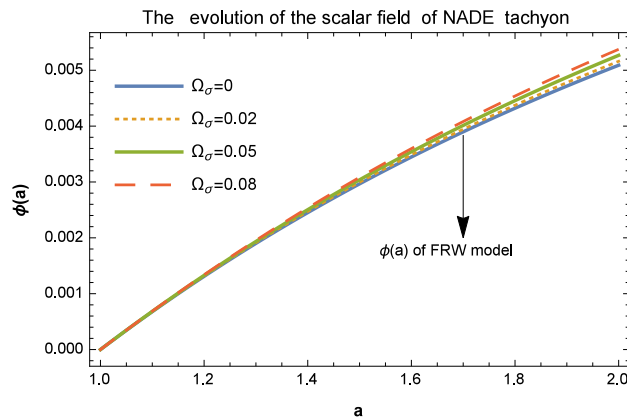


FIG. 9: The evolution of the NADE tachyon scalar field, Eq. (51), for different the anisotropy energy density parameter Ω_σ . Auxiliary parameters are $\Omega_\Lambda^0 = 0.72$, $b^2 = 0.02$, $n = 2$ and $\phi(1)=0$.

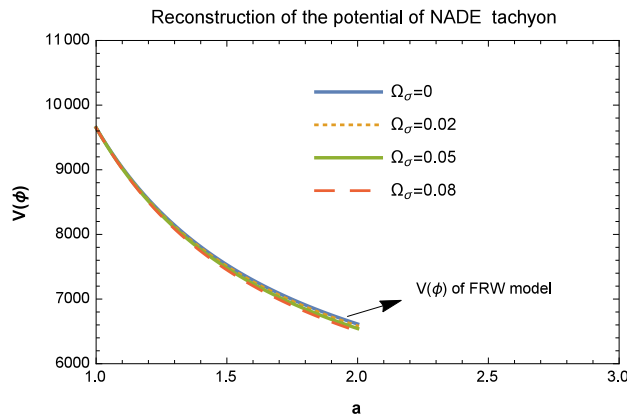


FIG. 10: The NADE tachyon potential, Eq. (49), versus the scale factor for different Ω_σ . Auxiliary parameters as in Fig. 9.

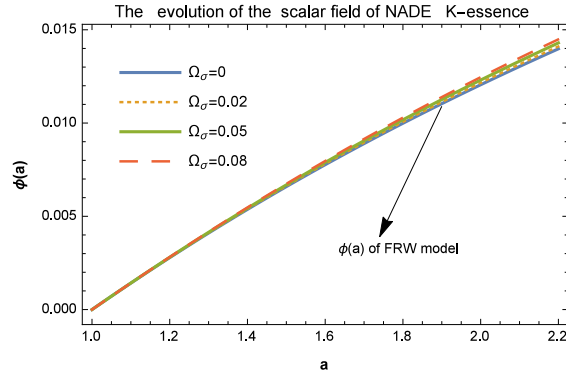


FIG. 11: The K-essence scalar field as function of the scale factor for the values of the Ω_σ . Auxiliary parameters are $\Omega_\Lambda^0 = 0.72$, $\phi(1) = 0$, $H_0 = 72$, $b^2 = 0.02$ and $n = 2$.

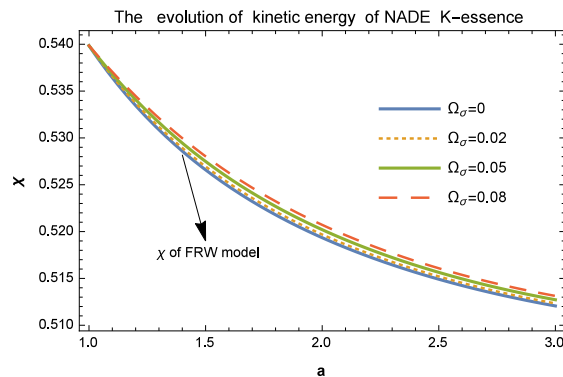


FIG. 12: The evolution of the new agegraphic K-essence kinetic energy $\chi = \dot{\phi}^2/2$ for different constant anisotropy Ω_σ . Auxiliary parameters as in Fig. 11.

tachyon potential $V(\phi)$ are plotted in Figs. 9 and 10, where again we have taken $\phi(a_0 = 1) = 0$ for the present time. Selected curves are plotted for different value of the anisotropy density parameter Ω_σ . From these figures we find out that ϕ increases with time while the potential $V(\phi)$ becomes steeper with increasing Ω_σ . This behavior is in agreement with the scaling solution $V(\phi) \propto \phi^{-2}$ obtained for the tachyon field corresponding to the power law expansion [41]. As the isotropic ($\Omega_\sigma = 0$) case the scalar field has a non-zero minimum which leads to an EoS parameter close to -1 for present time and near future. Again from Fig. 10 we find out the reconstructed scalar field has a same potential as the quintessence case.

C. K-essence reconstruction of NADE in BI

The K-essence scalar field model is also an interesting attempt to explain the origin of DE using string theory. Equating ω_K with the EoS parameter of NADE (39) one finds

$$\chi = \frac{2 - \frac{2}{3na}\sqrt{\Omega_\Lambda} + \frac{b^2}{\Omega_\Lambda}(1 - \Omega_\sigma)}{4 - \frac{2}{na}\sqrt{\Omega_\Lambda} + \frac{3b^2}{\Omega_\Lambda}(1 - \Omega_\sigma)}. \quad (52)$$

Using Eq. (52) and $\dot{\phi}^2 = 2\chi$, we obtain the new agegraphic K-essence scalar field as

$$\phi(a) - \phi(1) = \int_1^a \frac{1}{Ha} \sqrt{\left(\frac{4 - \frac{4}{3na}\sqrt{\Omega_\Lambda} + \frac{2b^2}{\Omega_\Lambda}(1 - \Omega_\sigma)}{4 - \frac{2}{na}\sqrt{\Omega_\Lambda} + \frac{3b^2}{\Omega_\Lambda}(1 - \Omega_\sigma)} \right)} da. \quad (53)$$

where we take $a_0 = 1$ for the present time. The evolution of the field and the reconstructed K-essence kinetic energy $\chi(\phi)$ are plotted in Figs. 11 and 12, where we have taken $\phi(a_0 = 1) = 0$ for simplicity. Note that in Fig. 11 the field increases with the increment of a . Obviously, the kinetic energy decreases with increasing the scale factor as shown in Figure 12. Figure 12 shows that $\chi(\phi)$ almost lies in the required interval (0.51, 0.54) from early epoch to the later time. The EoS parameter ω_K indicates that the accelerated universe can be obtained for this interval.

V. CONCLUSION AND DISCUSSION

In this work, we have investigated the different models of cosmology in an anisotropic universe, when we are using the scalar field models. In particular, we reconstructed the field equations of DE model in an anisotropic universe. Then we have reconstructed both the potentials and the kinetic energies corresponding to each model which describe quintessence, tachyon and K-essence cosmology. In addition, we have discussed main features by choosing different values of interacting parameter b^2 and different value of the anisotropy energy density parameter Ω_σ which are summarized as follows.

1. By using the Hubble radius as $L = H^{-1}$ IR cutoff, combinations of the HDE model and interacting scalar fields in anisotropic universe were implemented. We have obtained expressions for the scalar field and the potential for interacting HDE in BI model. The free parameters of cosmology have been evaluated in terms of the constants b^2 , Ω_σ and c^2 .
2. The EoS parameter ω_Λ of the NADE model in the BI models, can cross the phantom divide line ($\omega_\Lambda < -1$) at the present time, provided that $b^2 > 0.1$ which is compatible with the observations. By the way, the effect of various Ω_σ were negligible but as $a \rightarrow 0$, it was clear

that increasing of the Ω_σ cause to decrease the EoS parameter as shown in Figure 1. This type of behavior is consistent with the present observations. In the Figures 2 and 3 it have been illustrated, the Ω_Λ increased with the a increase but: I) increase of the Ω_σ caused the Ω_Λ increases with sharper slope. II) Increasing the coefficient coupling caused the early and final Ω_Λ values to ($a \ll (>>)$) increased (decreased) respectively III) at last, increase of n parameter caused the Ω_Λ parameter picked smaller value for the smaller scale factor i.e. $a \ll$. In addition, we have analyzed the outlooks for constraining the NADE in BI model by the Sandage-Loeb (SL) test. Therefore, the SL test can be used to distinguish the NADE in BI model from the Λ CDM model as shown in Fig. 4. Comparing the dynamical behaviour of the expansion expected in anisotropic universe with isotropic universe. To this propose, the evolution of Hubble parameter versus the redshift are shown in Figure 5. According to this model, the evolution of the accelerated expansion of the universe is speedy than the evolution of the isotropic model.

3. The new agegraphic quintessence scalar filed for a given Ω_σ , increases with increasing the scale factor, also, the curve was shifted to the larger value of ϕ with increasing Ω_σ as shown in Figure 6. For a given Ω_σ , potential $V(\phi)$ decrease with increasing the scale factor and the curve is shifted to the smaller values of $V(\phi)$ with increasing the Ω_σ as shown in Figure 7. Figure 8 shown which the fraction of potential per kinetic energy increase with the Ω_Λ increase and its magnitude increase with the Ω_σ increase for the smaller Ω_Λ .
4. The new agegraphic tachyon scalar filed for a given Ω_σ behave like the new agegraphic quintessence model as shown in Figures 9 and 10.
5. We have evaluated the interacting NADE versions of K-essence scalar field in BI models. These results have been shown in Figures 11 and 12. The new agegraphic K-essence scalar field for a given Ω_σ increases with increasing the scale factor. But its kinetic energy decreases. For a given scale factor, the new agegraphic K-essence scalar filed and kinetic energy increases with increasing Ω_σ .

Anyway, we have shown that the evolution of the NADE scalar filed and kinetic energy in anisotropic universe is larger than the evolution of the NADE scalar filed and kinetic energy in FRW space time. But its potential small. Finally we would like to mention that the aforementioned discussion in first part this work can be easily generalized to other choices of IR cut-off, namely, Ricci length scale and radius of the event horizon.

-
- [1] A.G. Riess, A.V. Filippenko, P. Challis, *et al.*, *Astron. J.* **116**, 1009 (1998).
 - [2] S. Perlmutter, G. Aldering, G. Goldhaber, *et al.*, *Astrophys. J.* **517**, 565 (1999).
 - [3] L. Susskind, *J. Math. Phys.* **36**, 6377 (1995).
 - [4] G.'t Hooft, *Int. J. Mod. Phys. D* **15**, 1587 (2006).
 - [5] S.D. Thomas, *Phys. Rev. Lett.* **89**, 081301 (2002).
 - [6] M. Gasperini, *et al.*, *Phys. Rev. D* **65**, 023508 (2002).
 - [7] M. Li, *Phys. Lett. B* **603**, 1 (2004).
 - [8] A.G. Cohen, D.B. Kaplan, A.E. Nelson, *Phys. Rev. Lett.* **82**, 4971 (1999).
 - [9] R.C. Myers, M.J. Perry, *Annals Phys.* **172**, 304 (1986).
 - [10] B. Wang, Y. Gong and E. Abdalla, *Phys. Lett. B* **624**, 141 (2005).
 - [11] Anjan A. Sen, D. Pavón, *Phys. Lett. B* **664**, 7 (2008).
 - [12] S.D.H. Hsu, *Phys. Lett. B* **594**, 13 (2004).
 - [13] D. Pavón and W. Zimdahl, *Phys. Lett. B* **628**, 206 (2005).
 - [14] E.N. Saridakis, *Phys. Lett. B* **660**, 138 (2008).
 - [15] J. Zhang, X. Zhang and H. Liu, *Eur. Phys. J. C* **52**, 693 (2007).
 - [16] R.G. Cai, *Phys. Lett. B* **657**, 228 (2007).
 - [17] H. Wei, R.G. Cai, *Eur. Phys. J. C* **59**, 99 (2009).
 - [18] H. Wei and R.G. Cai, *Phys. Lett. B* **660**, 113 (2008).
 - [19] H. Wei and R.G. Cai, *Phys. Lett. B* **663**, 1 (2008).
 - [20] J.-P. Wu, D.-Z. Ma and Y. Ling, *Phys. Lett. B* **663**, 152 (2008).
 - [21] I.P. Neupane, *Phys. Lett. B* **673**, 111 (2009).
 - [22] K. Karami, S. Ghaffari, J. Fehri, *Eur. Phys. J. C* **64**, 85 (2009).
 - [23] J. Zhang, X. Zhang, H. Liu, *Eur. Phys. J. C* **54**, 303 (2008).
 - [24] Y.H Li, J.Z. Ma, J.L. Cui, Z. Wang and X. Zhang, *Sci. China Phys. Mech. Astron.* **54**, 1367 (2011).
 - [25] E. Komatsu, *et al.*, *Astrophys. J. Suppl. Ser.* **180**, 330 (2009).
 - [26] E. Bertschinger, *Physica D* **77**, 354 (1994).
 - [27] I. Brevik, S.V. Pettersen, *Phys. Rev. D* **56**, 3322 (1997).
 - [28] I.M. Khalatnikov and A.Yu. kamenshchik, *Phys. Lett. B* **553**, 119 (2003).
 - [29] G.F.R. Ellis, *Cosmological models*, (2002).
 - [30] V. Fayaz, H. Hossienkhani, M. Amirabadi and N. Azimi, *Astrophys. Space Sci.* **353**, 301 (2014).
 - [31] H. Hossienkhani, A. Najafi and N. Azimi, *Astrophys. Space Sci.* **353**, 311 (2014).
 - [32] H. Hossienkhani and A. Pasqua, *Astrophys. Space. Sci.* **349**, 39 (2014).
 - [33] O. Bartolami and F. Gil, *Phys. Lett. B* **654**, 165 (2007).
 - [34] R. Bousso, *Rev. Mod. Phys.* **74**, 825 (2002).
 - [35] A. Sheykhi, *Phys. Rev. D* **84**, 107302 (2011).

- [36] M. Cataldo, N. Cruz, S. del Campo and S. Lepe, Phys. Lett. B **509**, 138 (2001).
- [37] N. Radicella and D. Pavón, JCAP, **10**, 005 (2010).
- [38] A. Sen, JHEP **10**, 008 (1999).
- [39] E.A. Bergshoeff, *et al.*, JHEP **0005**, 009 (2000).
- [40] T. Padmanabhan, Phys. Rev. D **66**, 021301 (2002).
- [41] E.J. Copeland, M.R. Garousi, M. Sami and S. Tsujikawa, Phys. Rev. D **71**, 043003 (2005).
- [42] F. Piazza and S. Tsujikawa, JCAP **07**, 004 (2004).
- [43] T. Chiba, T. Okabe, M. Yamaguchi, Phys. Rev. D **62**, 023511 (2000).
- [44] B. Wang, J. Zang, Ch.Y. Lin, E. Abdalla, S. Micheletti, Nucl. Phys. B **778**, 69 (2007).
- [45] M. Li, X.D. Li, S. Wang and X. Zhang, JCAP **0906**, 036 (2009).
- [46] J.F. Zhang, Y.H. Li and X. Zhang, Eur. Phys. J. C **73**, 2280 (2013).
- [47] J. Zhang, L. Zhang and X. Zhang, Phys. Lett. B **691**, 11 (2010).
- [48] D.N. Spergel, R. Bean, O. Doré *et al.*, Astrophys. J. Suppl. **170**, 377 (2007).
- [49] J.R. Gott, M.S. Vogeley, S. Podariu and B. Ratra, Astrophys. J. , **549**, 1 (2001).